Desalination and Water Treatment
www.deswater.com
doi: 10.1080/19443994.2016.1186565

57 (2016) 27700–27709
December

Preparation and characterization of microfiltration apatite membrane over low cost clay-alumina support for decolorization of dye solution

Ganesh C. Sahoo[a], Rupa Halder[a], Ilyes Jedidi[b], Abdallah Oun[b], Hassen Nasri[b], Piyali Roychoudhurry[a], Swachchha Majumdar[a], Sibdas Bandyopadhyay[a], Raja Ben Amar[b,*]

[a]*CSIR-Central Glass & Ceramic Research Institute, 196 Raja S. C. Mullick Road, Kolkata 700032, India, emails: gcsahoo07@gmail.com (G.C. Sahoo), rupa.chemical@gmail.com (R. Halder), piyali.hit@gmail.com (P. Roychoudhurry), swachchha@gmail.com (S. Majumdar), sibdas2013@gmail.com (S. Bandyopadhyay)*
[b]*Laboratory of Material Science and Environment, Faculty of Science of Sfax, University of Sfax, Route de la Soukra Km4, Sfax 3000, Tunisia, emails: ilyesjedidi@yahoo.com (I. Jedidi), ounabdallah@yahoo.fr (A. Oun), nasrihassen@gmail.com (H. Nasri), raja.rekik@fss.rnu.tn (R. Ben Amar)*

Received 15 October 2015; Accepted 8 April 2016

ABSTRACT

Apatite material obtained from natural sources of Tunisian mineral has been used for the development of membrane over clay–alumina-based microporous supports. For this purpose, supports of single-channel and 19-channel circular configurations were used. The apatite powder used for membrane preparation had average pore diameter of 4.02 μm. Coating formulation has been optimized to obtain stable suspension. Powder loading of 4 wt.% was found as optimum for obtaining a proper microfiltration membrane with 0.2 μm pore diameter. Single-channel membrane was used for characterization. The application to color removal from synthetic reactive dye solution was performed using membrane with 19-channel configuration. An average water flux of 200 and 80 l/m^2 h was obtained for 19-channel support and membrane, respectively, in laboratory scale setup. Reactive red dye removal from synthetic dyeing solution was achieved up to 99%. Resulting saturated membrane was successfully regenerated using H_2O_2 at various concentrations and contact time. Color separation efficiency of the membrane (g/m^2) has been evaluated as an indicator of membrane regeneration. Moreover, apatite membrane-based separation of reactive red dye has been compared with adsorption using the apatite powder followed by membrane separation. Apatite membrane-based separation was found to be more efficient compared to adsorptive separation using apatite powder.

Keywords: Apatite membrane; Clay–alumina support; Color removal; Membrane regeneration; Adsorption

1. Introduction

Many efforts to achieve economical and efficient membranes for various uses have resulted in a selection of new materials, improvement in membrane preparation techniques, and increase in the number of applications [1,2]. At present, the interest is derived toward inorganic membranes due to their superior permeability–selectivity combination, high self-life,

---

*Corresponding author.

and suitable performance at high temperature or corrosive environment compared to polymeric membranes [3].

A thin separation layer and a porous support characterize the majority of inorganic membranes employed in separation processes with a pressure gradient. In general, the commercial microfiltration membranes have a top layer based on zirconium, titania, or alumina deposited on carbon or alumina support [4–6]. Thus, industrial membrane production uses a limited choice of materials. Consequently, ceramic membranes have a high price primarily due to use of high-purity materials for the preparation of supports and coating layer in addition to relatively high sintering temperature needed for strong bonding between membrane and support. Attempts to find new porous ceramic materials at low price and needing low thermal treatment temperatures have been reported in the literature [7–10]. Thus, different strategies were followed to prepare ceramic membranes at low cost. Some researchers reported on the use of active layers and supports from the same material such as clay, natural apatite, mineral coal fly ash, and carbon as low-cost materials for the preparation of microfiltration and ultrafiltration membranes [11–15]. The prepared membranes showed very good separation properties when applied to different industrial wastewaters [16–22]. Other researchers mixed clay with alumina to prepared low-cost macroporous supports with high mechanical performances and with tunable porosity [7,10,23]. These supports were successfully scaled up to 1.2 m long multichannel configuration [24].

This study describes the elaboration of ceramic membrane over mono- and multichannel clay–alumina supports based on Tunisian natural apatite. These membranes were used for the treatment and the decolorization of reactive dye solutions and compared with adsorption using the powder.

2. Materials and methods

2.1. Natural apatite characterization

Apatite powder used for the preparation of the microfiltration layer is coming from Tunisian Phosphate Company. Different techniques were used for the characterization. So particle size was analyzed using Mastersizer Hydro 2000MU (Malver Instruments Ltd, UK). The powder morphology as well as the microstructure of samples was determined using HiTASHI Scanning Electron Microscopy (SEM). The chemical composition (wt.%) of the apatite powder was determined by chemical analysis, and apatite characteristics was obtained from IR spectral analysis. IR transmittance spectra of the grounded sample were obtained in the 4,000–400 cm^{-1} region on a Nicolet Nexus FT-IR spectrometer. The XRD patterns were recorded using XRD instrument (Philips PW-1730, USA, Radiation CuKα, $\lambda = 0.15418$ nm). Thermogravimetric analysis (TGA) and differential scanning calorimetry (DSC) (NETZSCH STA 449F3 JUPITER, Germany) were carried out with approximately 22 mg of apatite. Temperature varied from 0 to 1,000°C at a rate of 5°C/min, under air.

2.2. Membrane elaboration

The objective of this part is to develop a microfiltration layer from natural apatite on a macroporous clay–alumina support in mono- and multichannel configuration having, respectively, 150 mm (OD/ID = 9 mm/6 mm) and 200 mm length (34 mm OD, 19-channels, and each of 4.2 mm nominal diameter). Both the supports have 1.1 μm averages pore diameter and a porous volume of 42% [24].

For preparing the microfiltration layer, a deflocculated slip was obtained by mixing natural apatite powder, PVA solution as binder and distilled water as solvent. The rheological behavior of the slips was determined according to the protocol described in a previous work [25,26] (Table 1).

The slip casting process applied to coat both support configurations to prepare microfiltration membrane is described elsewhere [25] and consists of the following steps:

(1) Preparation of suspension of the apatite powder in the aqueous solution.
(2) De-agglomeration of the coating slurry by agitation under ultrasounds using ultrasonic bath for 15 min.
(3) Addition of binder (12 wt.% aqueous solution of PVA) and homogenization by slow magnetic stirring.
(4) For coating of the support tubular membranes at room temperature using dip-coating method, the tube was closed at one end and filled with the coating suspension through open end and kept for 10 min (optimal duration).
(5) Drying for 24 h at room temperature.

The thermal treatment program for membrane sintering was established from the TGA carried out on apatite samples and dried unsupported green membrane using a thermogravimetric analyzer (TGA) and differential scanning calorimeter (DSC), simultaneous DSC-TGA using 2960 TA instrument. The apatite

Table 1
Three different compositions of the slips

Slip code	Apatite powder	PVA solution	Water
Slip I	2 wt.%	40 wt.% (12 wt.% in water)	58 wt.%
Slip II	4 wt.%	40 wt.% (12 wt.% in water)	56 wt.%
Slip III	6 wt.%	60 wt.% (12 wt.% in water)	34 wt.%

sample was heated from room temperature to 1,000˚C at a rate of 5˚C/min under static atmospheric conditions, and unsupported membranes were heated from 50 to 900˚C at the rate of 10˚C/min in air.

Sintering was performed at a temperature of 750˚C during 3 h. A temperature plateau at 250˚C for 2 h was maintained in order to complete elimination of the binder (PVA) present in the slip with a relatively slow heating rate (1˚C/min), in order to avoid the formation of cracks and defects on the layer.

2.3. Membrane characterization

The porosity and the average pore diameter of the final material were determined by mercury intrusion porosimetry (Micrometrics Autopore II 9220 V3.05). The SEM analysis was used to measure the membrane thickness and to check the surface morphology of the layer for the presence of any crack or defect.

2.4. Membrane application

Water permeability of multichannel coated tube and support element were performed in cross-flow membrane filtration (CMF) mode at a temperature of 25˚C using a laboratory scale setup. Pressure effect and duration of filtration on membrane flux were studied. Transmembrane pressure (TMP) that ranged between 0.5 and 2.0 bar which corresponds to the microfiltration range was used. The total active area of the multichannel membrane was 42.0×10^{-3} m. Membranes were preconditioned by immersion in deionized water for at least 24 h prior to the permeability tests. The duration of each tests ranged from 1 to 7 h, and each run was conducted twice for repeatability study.

Apatite microfiltration membrane coated over 19-channel support was tested for the removal of color from synthetic dyeing solution of reactive red dye. For that, 5 L of solution was prepared by dissolving 0.1 g of reactive red dye and 15 g of NaCl in distilled water to have similar conditions that of textile dyeing effluent. Experiments were carried out at 1.0 bar TMP. Color was measured in a UV–visible spectrophotometer (Cary 50 Bio, Varian, Australia) and pH, conductivity, and salinity using a multi-parameter (HACH, USA). The membrane regeneration study was carried out after each experiment using H_2O_2 at various concentrations in CMF mode at a pressure of 0.5 bar and temperature of 30˚C.

2.5. Adsorption of dye using apatite powder

Adsorptive separation using apatite powder followed by microfiltration was conducted in laboratory scale. The feed for color removal study was formulated by dissolving reactive red dye of 0.1 g in 5 l. The microfiltration study was conducted using clay–alumina-based 19-channel ceramic support tube. The TMP was maintained at 1.0 bar. Color concentration before and after treatment was measured using UV–visible spectrophotometer (Varian Pvt. Ltd, Australia). In this study, the natural apatite powder was used without further treatment as well as powder calcined at 750˚C as adsorbents with the dose variation from 1 to 5 g/l. The total sample volume and operational time were five liters and 6 h, respectively.

3. Results and discussion

3.1. Apatite powder characterization

The chemical composition of natural apatite powder was determined through chemical analysis of the powder. Calcium and phosphorous are the major constituents and minute amount of fluoride (0.1 wt.%) as evident from analysis data shown in Table 2.

The natural apatite coarse mineral was crushed into powder, and particle size distribution was analyzed using Mastersizer. Fig. 1 shows that particle size varied from 0.3 to 25 μm. An average particle size ($d_{0.5}$) of 4.02 μm which is suitable for MF membrane preparation was obtained. Scanning electron microscopic analysis of the powder showed that particles had an oval shape in general but with heterogeneous distribution. Zooming on the surface of a particle showed its porous texture. Indeed, natural apatite powder has a specific surface area of 26.01 m/g,

Table 2
Chemical composition of natural apatite powder

Constituent	P_2O_5	CaO	SiO_2	Al_2O_3	Fe_2O_3	MgO	CO_2	C_{org}	SO_3	Cl^-	F^-
Wt.%	28.92	49.14	3.10	0.58	0.26	0.70	0.90	0.90	3.21	0.10	0.10

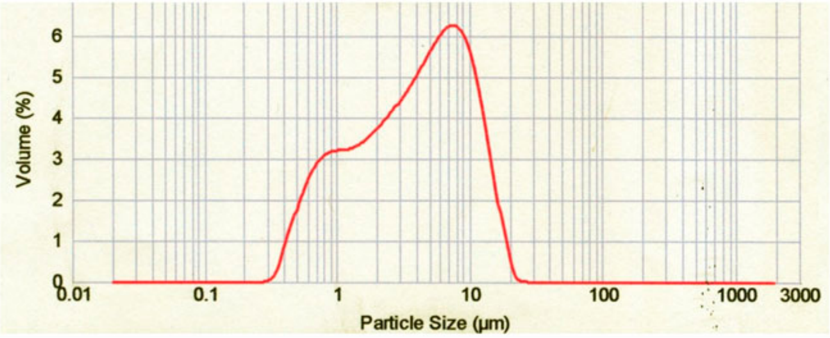

Fig. 1. Particle size distribution of Tunisian natural apatite powder.

obtained from BET_M analysis (ASIMP-LP2, Quantachrome Instruments, USA).

Fig. 2 illustrates IR spectrum of the natural apatite sample. Apatite characteristic bands appear clearly in the spectrum. 3,570 cm^{-1} band is characteristic for stretching and vibrational modes of the OH^- ions. Characteristic frequencies derived from PO_4^{3-} group are depicted by bands at 1,110, 1,037, 964, 607, 565, and 469 cm^{-1}. In addition, the band characteristics of CO_3^{2-} ion (876-1, 420-1, 463) are present in the IR spectrum. The range of bands from 1,800 to 2,400 cm^{-1} results from the diamond in the spectrometer [27,28].

Fig. 3 represents the X-ray diffractogram of the natural apatite powder. It shows characteristic peaks for apatite. No other phases were detected on the XRD of the sample. The XRD pattern can be indexed in the hexagonal system; the space-group is $P6_3/m$ [25]. Major d-spacing values (Å) obtained 2.78252,

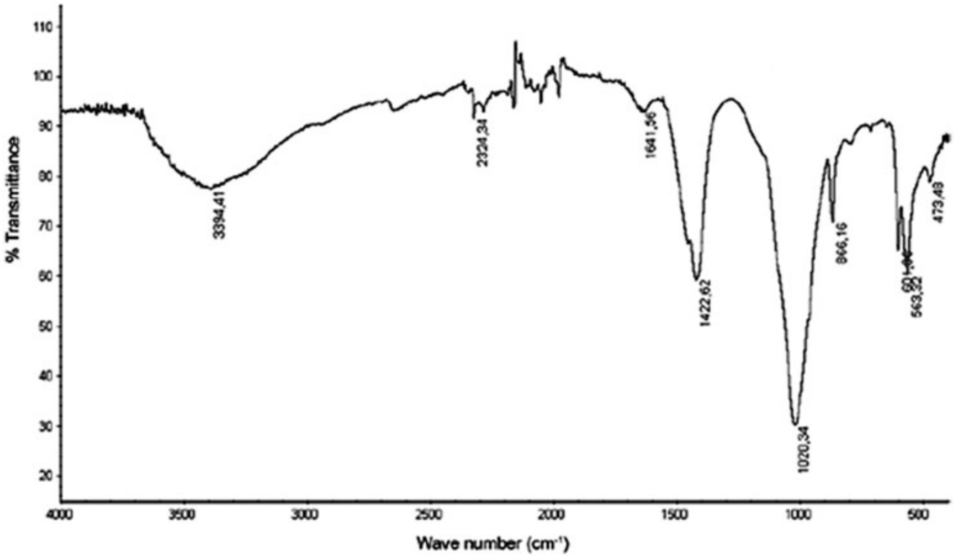

Fig. 2. IR spectrum of natural apatite powder.

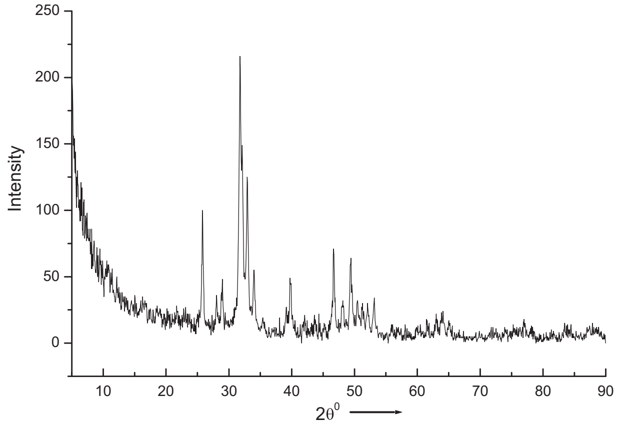

Fig. 3. X-ray diffractogram of the apatite powder.

2.68158, and 3.43075 at $2\theta^\circ$ values of 32.1701, 33.4159, and 25.9721, respectively, corresponds to fluorapatite nature of the apatite powder [28–30].

DTA/TG analysis graph of the powder was done. Analysis shows a glass transition temperature (Tg) at 610–680 °C and mass change of 9 wt.%. Accordingly, 750 °C was selected as sintering temperature of apatite-coated membrane.

3.2. Slip characterization

The effect of the percentage of apatite powder and PVA solution on behavior of slurry was studied by measuring rheological properties viz. viscosity and shear stress using rheometer (Lamy TVe-05) (Figs. 4(a) and (b)). The rheological behavior was unchanged for PVA percentages ranging between 40 and 60% and apatite percentage between 4 and 6%. The slips have a plastic behavior of Bingham [31], controlled by the presence of PVA. The value of the limiting shear stress was 84 Pa for 60% of PVA. Such behavior permits to maintain particles in a stable suspension. Slip I with 2 wt.% solid loading has different rheological behavior and has low viscosity. So it was not suitable for homogeneous coating and was not processed further.

3.3. Characterization of unsupported membrane

Unsupported green membranes were characterized by DTA/TG analysis of the dried slips II and III and showed mass change of −1.61 and −1.86%, respectively, within the temperature range of 740 °C. Results showed similar exothermic behavior of the slips with no sharp peak and weight loss due to elimination of organic binder. Unsupported membranes obtained after sintering of the green and dried unsupported membranes of slips II and III at 750 °C were also analyzed for pore size distribution using Hg-intrusion

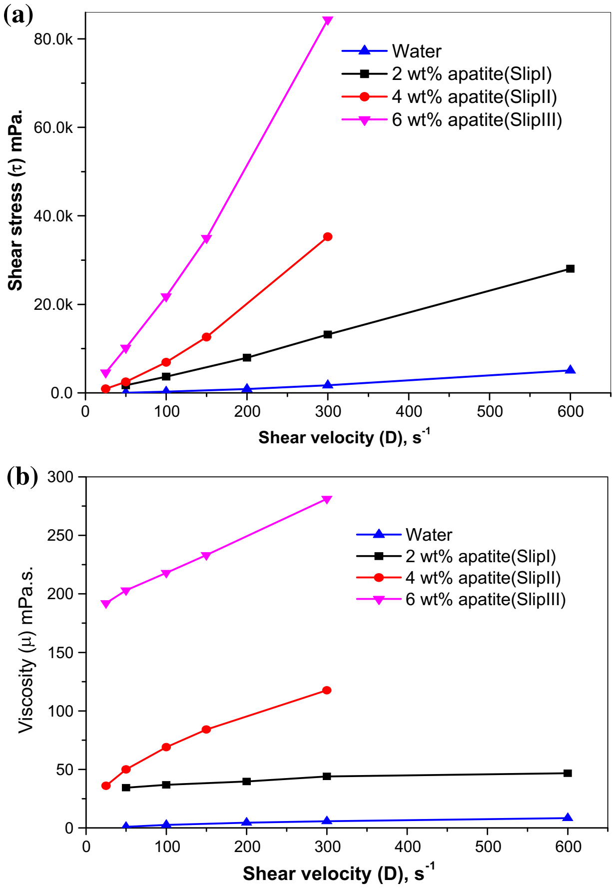

Fig. 4. Evolution of the shear stress (τ) (a) and the viscosity (μ) (b) vs. deformation for 12% of the PVA at different % of apatite.

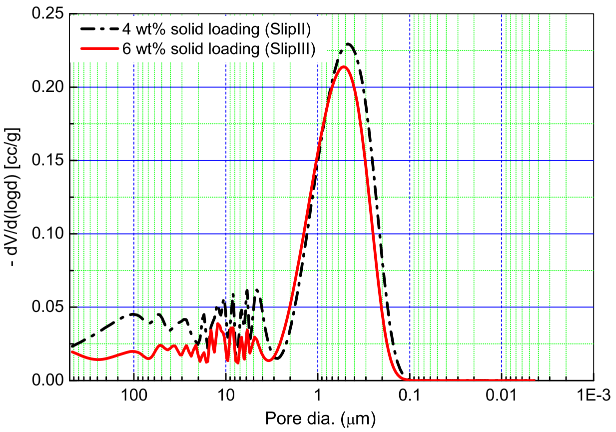

Fig. 5. Hg-intrusion pore size distribution up to 50,000 psi of natural apatite-based unsupported membranes of slips II and III fired at 750 °C for 3 h.

porosimetry as shown in Fig. 5. Pore size distribution data show that the unsupported membranes are in the microporous range and pore diameter varies from 0.1 to 2.0 μm.

3.4. Membranes characterization

3.4.1. Texture

SEM image and EDX analysis of 4–6 wt.% apatite-coated membrane over single-channel porous clay–alumina tube are shown in Fig. 6. SEM analysis of micrographs of 4 wt.% apatite (Slip II)-coated membrane shows homogeneous membrane surface with less than 0.2 μm pore diameter (Fig. 6(a)) and membrane thickness of 3–4 μm. While 6 wt.% apatite (Slip III)-coated membrane shows 4–5 μm membrane thickness (Fig. 6(b)), EDX analysis of the membrane surface shows abundant quantity of Ca with Si, Na, K, P etc. (Fig. 6(c)). Similar microstructure of SEM images was obtained from coated layer (Slip II) on 19-channel porous clay–alumina supports and found the layer was homogeneous, cracks free, and firmly adhered to the clay–alumina porous material. Transverse view of SEM image and line EDX analysis of the image showed a regular membrane thickness of 10 μm and Ca and P were the abandon elements.

The texture of the membrane seems depending on the type of the support and on its configuration in particular in terms of membrane layer thickness. The average membrane thickness of 4–10 μm found in this study, respectively, for single-channel and multichannels membranes is lower than that found in the case of single channel for others MF membranes based on apatite material. Masmoudi et al. [15] reported that a thickness of 32.5 μm was observed with 0.5 μm MF natural apatite membrane over cordierite support was prepared. The elaboration of 0.2 μm MF synthesized hydroxyapatite membrane over natural apatite support produced a thickness of 45 μm. However, the use of natural hydroxyapatite instead of synthesized hydroxyapatite as MF layer showed a thickness of 10 μm [25] which is in the same order of magnitude as found in this study.

3.4.2. Pore size and porosity

The distribution of the membrane pores diameter was determined by mercury intrusion porosimetry. The average pore diameter and porous volume of the active layer and the support are about 0.28 μm and 42%, respectively (Fig. 7). Pore size value indicates that the prepared membrane can be utilized for microfiltration applications.

3.5. Water permeability

Pressure effect on permeate flux showed that the increase in permeate flux with pressure was much higher for support compared to the membrane. This result is expected since the addition of the layer with smaller pore size provides additional hydraulic resistance to the mass transfer. Also, relating to the physical properties, clay–alumina having high hydrophilicity may play an important role in the flux behavior against the variation of pressure. On other hand, effect of duration on permeate flux was not significant. Steady flux of 200 l/m^2 h remained higher for support against 80 l/m^2 h for membrane. This result shows that the prepared membrane has considerable stability [9,10].

3.6. Color removal study

Reactive dye color ($\lambda_{\max} = 531$ nm) removal capacity of apatite membrane over 19-channel clay–alumina porous support was performed in laboratory scale setup of 5 l capacity at 1.0 bar TMP. There is no significant difference in salinity (3.0 g/l), conductivity (5,500 μs/cm), and pH (6.4) between feed and permeate but a rapid reduction in color has been observed in both the phases as evident from the Fig. 8. It can be observed that at first, there is a quasi-stability of flux during the first two hours and then a decrease in flux. After three hours, the flux stabilized again. Compared to the water flux, it can be seen that there is a sudden decrease in initial permeate flux from 75 to 60 l/m^2 h. This decrease is attributed to the formation of dye molecule layer on the membrane surface. Flux remained stable until saturation. Then, the flux declined may be due to intrusion of the dye molecules into the membrane pores [32]. It is in accordance with the retention behavior of color in feed tank. This indicates cake filtration at the membrane surface followed by depth filtration throughout the membrane. Indeed, the color retention increased drastically to reach almost 99% after two hours and then stabilized due to the saturation of the active layer. While, for permeate, it was seen that quasi-stable retention was obtained after one hour. Thus, in this case, adsorption plays an important role in color reduction. It was observed that there was no significant change in salinity at pH 6.4 throughout the experiment. This is may be due to sintering of the apatite membrane at higher temperature (750˚C).

The stabilized permeate flux of 60 l/m^2 h obtained at 1 bar TMP is almost the same as that obtained with UF membrane synthesized completely (for the support

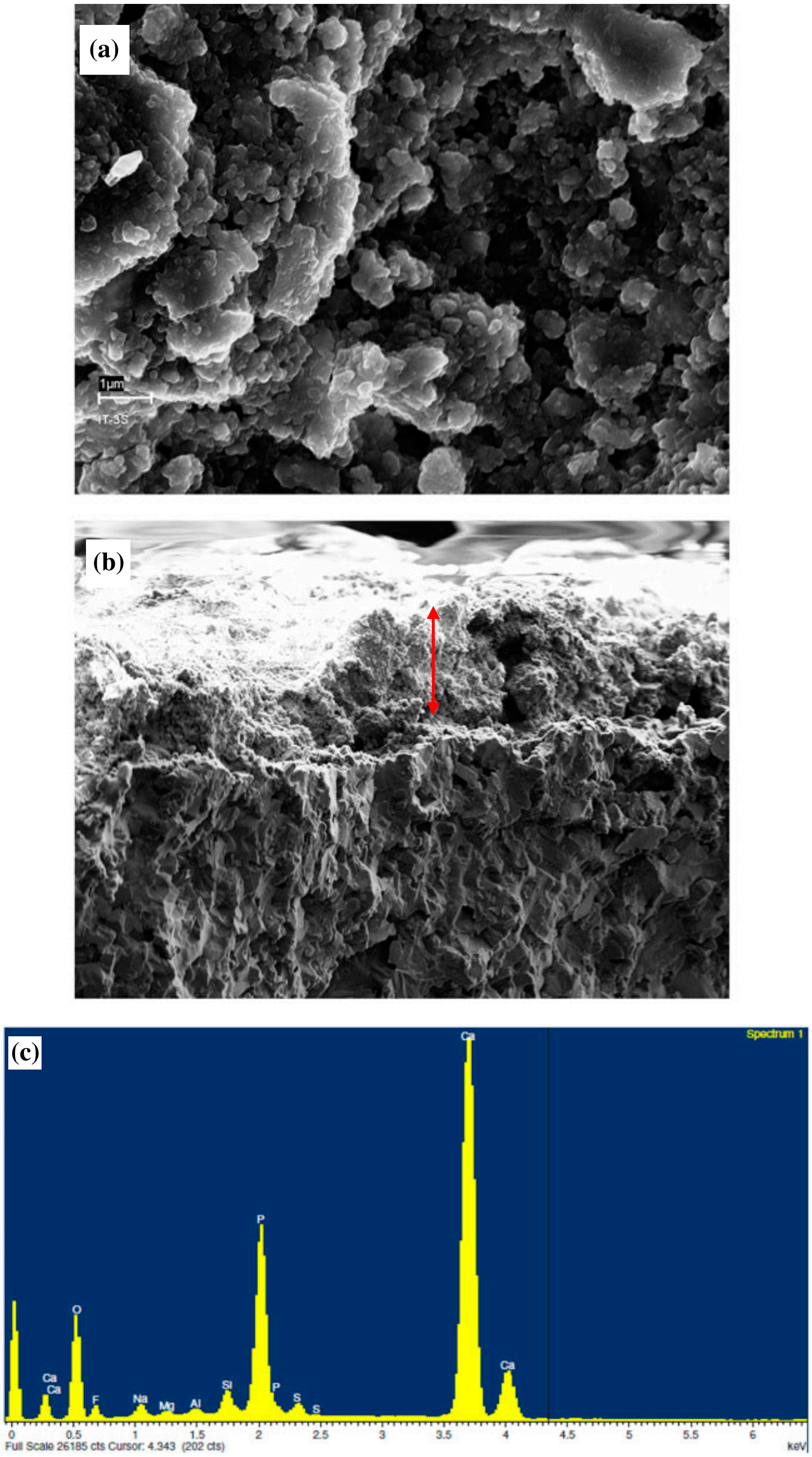

Fig. 6. SEM photographs of natural apatite-coated membrane over single-channel porous clay–alumina support tube: (a) surface view of Slip II-coated membrane, (b) transverse view of Slip III-coated membrane, and (c) EDX analysis of Slip III-coated membrane.

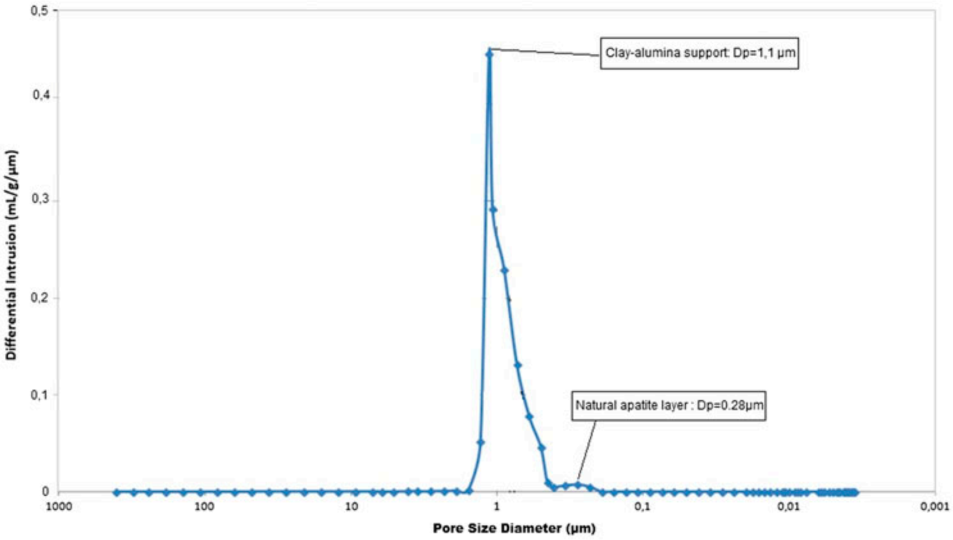

Fig. 7. Mercury intrusion porosimetry analysis of natural apatite membrane on clay–alumina 19-channel membrane support.

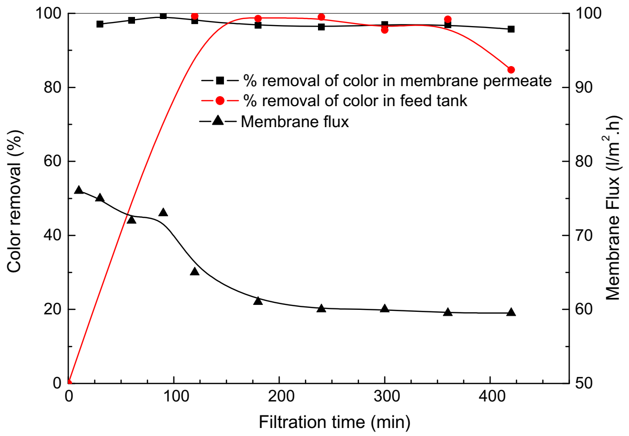

Fig. 8. Color removal using natural apatite membrane over 19-channel clay–alumina support in cross-flow mode at 1 bar TMP.

and the active layer) from mud of hydrocyclone laundries phosphates (derived from Tunisian phosphate transformation industry) when applied to the treatment of industrial textile wastewater at a TMP of 5 bar. A total removal of color was also observed in this case [33]. By referring to the literature, it seems that apatite-based membranes exhibited better performances than commercial ceramic membranes. Indeed, G. Masmoudi et al. [34] compared MF and UF performances using, respectively, alumina and titania multichannel membrane during the treatment of industrial dyeing effluent. They found that the MF led to a color removal of 46% and drastically a decrease in the permeate flux due to the membrane fouling, whereas the UF exhibited lower membrane fouling and higher color retention of 64%.

3.7. *Color removal study by adsorption followed by microfiltration process using natural apatite as adsorbent*

Fig. 9 shows that color removal percentage increased with the increase in the natural apatite powder dosing but beyond 5 g/l, there was no significant change in color removal data. Steady membrane flux was observed after 4 g/l of natural apatite dosing. The calcined NA shows better removal, and the maximum

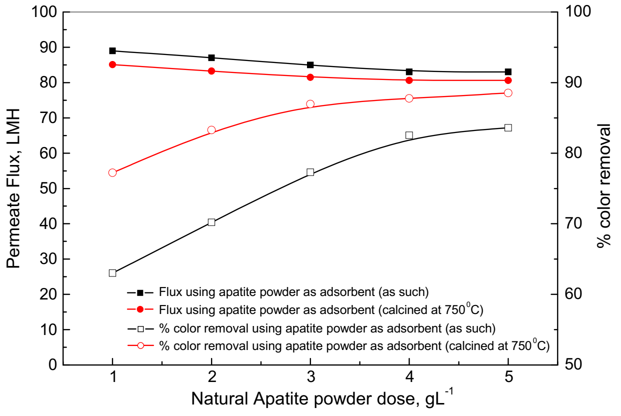

Fig. 9. Color removal study using apatite powder and calcined apatite powder as adsorbents followed by cross-flow microfiltration at 1 bar TMP.

color removal achieved was 88%. It shows that apatite-based membrane separation (99%) is much higher compared to adsorptive separation using the same apatite powder. Steady permeate flux of 83 l/m^2 h was obtained. Flux using adsorbent *in situ* was closer to that of membrane flux (80 l/m^2 h).

3.8. Membrane regeneration

Membrane regeneration study was carried out after every color removal study using H_2O_2 at various concentrations. Fig. 10 shows dye removal efficiency of the regenerated membrane at various conditions. Dye concentrations at zero time in the graph are the initial concentrations in feed solution. Membrane regeneration was more effective for higher concentration of H_2O_2 and duration of treatment. Optimum regeneration conditions obtained was 1% (v/v) of H_2O_2 for 7-h treatment time. Indeed, the data were generated in duplicate and were presented as average.

Membrane separation efficiency for dye was calculated based on the amount of dye (g) adsorbed/separated per unit surface area (m^2) of the membrane. For this, differences of initial and final concentration in the feed were determined. Taking into account the given absorbance against concentration (ppm), the volume of the feed (5 l), and the effective filtration area of the membrane, the amount of adsorbed color was expressed in terms of g/m^2. More than 60% of initial capacity (1.1 g/m^2) could be regenerated even after several separation cycles.

The aim of the experiments in Sections 2.4 and 2.5 were to understand whether adsorption alone or adsorption and membrane filtration play the role in color removal. A comparative study has been made using (i) apatite membrane-based separation (Section 2.4) and (ii) apatite powder *in situ* adsorption followed by membrane filtration (Section 2.5). Two kinds of apatite powders have been used, viz. powder as such and powder calcined to 750°C. It shows that apatite membrane separation (99%) was much higher compared to when its powder was used *in situ* (Section 3.7). It is evident that both adsorption and membrane filtration play important role in color removal in this study.

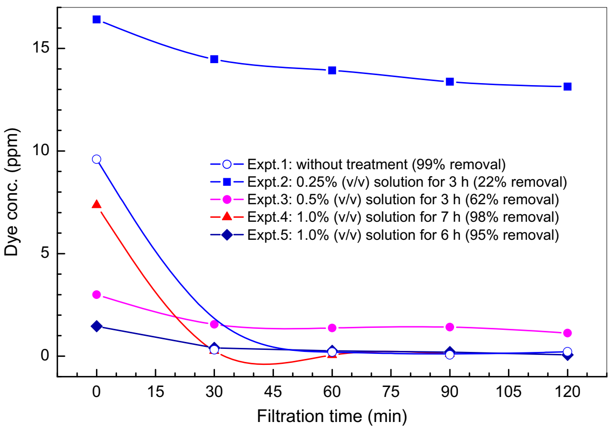

Fig. 10. Effect of regeneration conditions on color removal (reactive red dye) using H_2O_2.

4. Conclusion

Natural apatite membrane was developed over low-cost clay–alumina ceramic membrane support tube of single-channel and 19-channel circular configuration. Membrane was characterized and subjected to color removal showing encouraging results. Comparative study on apatite membrane separation and adsorptive separation using the apatite powder showed that the former was more effective in color separation. Membrane separation efficiency could be regenerated to a large extent. This observation may be extended for scaling up for treatment of textile industry wastewater.

Acknowledgements

Financial support from DST, New Delhi, Government of India (DST Sanction No. INT/Tun/P-1(9)/2009, dated 26.03.2012) and Government of Tunisia is highly acknowledge through the Indo-Tunisia Programme of Co-operation in Science & Technology.

References

[1] W.J. Koros, R. Mahajan, Pushing the limits on possibilities for large scale gas separation: Which strategies, J. Membr. Sci. 175 (2000) 181–191.

[2] A.F. Ismail, L.B. David, A review on the latest development of carbon membranes for gas separation, J. Membr. Sci. 193 (2001) 1–18.

[3] H.P. Hsieh, Inorganic Membranes for Separation and Reaction, Elsevier, New York, NY, 1996.

[4] S. Khemakhem, R. Ben Amar, R. Ben Hassen, A. Larbot, A. Ben Salah, Elaboration de supports Tubulaires à base demarne silteuse tunisienne et d'une membrane de microfiltration en ZrO_2, l'industrie céramique et verrière, 997 (2004) 133–138.

[5] S. Masmoudi, H. Feki, A. Larbot, R. Ben Amar, Elaboration and characterization of new ceramic ultrafiltration membrane with hydroxyapatite, Ceram. Int. 33 (2007) 337–344.

[6] S. Khemakhem, R. Ben Amar, A. Larbot, Synthesis and characterization of a new inorganic ultrafiltration membrane composed entirely of Tunisian naturally Illite clay, Desalination 206 (2007) 210–214.

[7] S. Sarkar, S. Bandyopadhyay, A. Larbot, S. Cerneaux, New clay–alumina porous capillary supports for filtration application, J. Membr. Sci. 392–393 (2012) 130–136.

[8] S. Khemakhem, A. Larbot, R. Ben Hassen, R. Ben Amar, L. Cot, A.H. Ben Salah, Fabrication of mineral supports of membranes for microfiltration/ultrafiltration from Tunisian clay, Ann. Chim. Sci. Mat. 31 (2006) 169–181.

[9] S. Khemakhem, R. Ben Amar, A. Larbot, New ceramic microfiltration membranes from Tunisian natural materials: Application for the cuttlefish effluents treatment, Ceram. Int. 35 (2009) 55–61.

[10] M. Khemakhem, S. Khemakhem, S. Ayedi, R. Ben Amar, Study of ceramic ultrafiltration membrane support based on phosphate industry sub-product: Application for the cuttlefish conditioning effluents treatment, Ceram. Int. 37 (2011) 3617–3625.

[11] A.S. Mukasyan, C. Costello, K.P. Sherlock, D. Lafarga, A. Varma, Perovskite membranes by aqueous combustion synthesis: Synthesis and properties, Sep. Purif. Technol. 25 (2001) 117–126.

[12] S. Chemlal, M. Sghyar, M. Rafiq, A. Larbot, L. Cot, Elaboration de membranes de spinelles de cobalt $CoAl_2O_4$ et de spinelle de manganèse $MnAl_2O_4$ pour l'ultrafiltration, Ann. Chim. Sci. Mater. 25 (2000) 577–582.

[13] I. Jedidi, S. Saidi, A. Larbot, R. Ben Amar, New ceramic microfiltration membranes from mineral coal fly ash, J. Hazard. Mater. 172 (2009) 152–158.

[14] I. Jedidi, S. Saïdi, S. Khemakhem, A. Larbot, N.E. Ammar, A. Fourati, A. Charfi, A. Ben Salah, R. Ben Amar, Elaboration of new ceramic microfiltration membranes from mineral coal fly ash applied to waste water treatment, J. Hazard. Mater. 172 (2009) 152–158.

[15] S. Masmoudi, R. Ben Amar, A. Larbot, H. El Feki, A. Ben Salah, L. Cot, Elaboration of inorganic microfiltration membranes with hydroxyapatite applied to the treatment of wastewater from sea product industry, J. Membr. Sci. 247 (2005) 1–9.

[16] P. Bhattacharya, S. Ghosh, S. Majumdar, S.N. Roy, S. Bandyopadhyay, Ceramic membrane based microfiltration for treatment of highly contaminated tannery wastewater, Environ. Eng. Manag. J. 14 (2015) 2139–2148.

[17] P. Bhattacharya, S. Sarkar, S. Ghosh, S. Majumdar, A. Mukhopadhyay, S. Bandyopadhyay, Potential of ceramic microfiltration and ultrafiltration membrane for treatment of grey water for an effective reuse, Desalin. Water Treat. 51 (2013) 4323–4332.

[18] P. Bhattacharya, S. Ghosh, S. Sarkar, S. Majumdar, S. Bandyopadhyay, Effectiveness of biosorption assisted microfiltration process for treatment of domestic wastewater, Biorem. J. 15(4) (2011) 206–217.

[19] P. Bhattacharya, S. Dutta, S. Ghosh, S. Vedajnananda, S. Bandyopadhyay, Cross-flow microfiltration using ceramic membrane for treatment of sulfur black effluent from garment processing industry, Desalination 261 (2010) 67–72.

[20] S. Khemakhem, R. Ben Amar, R. Ben Hassen, A. Larbot, A. Ben Salah, New ceramic membranes for tangential waste-water filtration, Desalination 167 (2004) 19–22.

[21] S. Khemakhem, A. Larbot, R. Ben Amar, Study of performances of ceramic microfiltration membrane from Tunisian clay applied to cuttlefish effluents treatment, Desalination 200 (2006) 307–309.

[22] S. Masmoudi, A. Larbot, H. Feki, R. Ben Amar, Use of ultrafiltration membranes with apatite for the treatment of cuttlefish effluent, Desalination 200 (2006) 335–336.

[23] S. Khemakhem, R. Ben Amar, R. Ben Hassen, A. Larbot, A. Ben Salah, Production of Tubular ceramic membranes for microfiltration and ultrafiltration, Ind. Ceram. 24 (2004) 113–116.

[24] T. Dey, G.C. Sahoo, S.N. Roy, S. Bandyopadhyay, Studies on pre-treatment of seawater using tubular ceramic MF membrane of 19-channel configuration, Int. J. Sci. Res. Publ. 3(10) (2013) 1–5.

[25] S. Masmoudi, A. Larbot, H. El Feki, R. Ben Amar, Elaboration and properties of new ceramic microfiltration membranes from natural and synthesised apatite, Desalination 190 (2006) 89–103.

[26] H. Nasri, S. Khemakhem, R. Ben Amar, Physico-chemical study of coating formulation based on natural apatite for the elaboration of microfiltration membrane, Period. Polytech. 58 (2014) 171–178.

[27] B.O. Fowler, Infrared spectra of apatite, in: W.E. Brown, R.A. Young (Eds.), International Symposium on Structural Properties of Hydroxyapatite and Related Compounds, Gaithersburg, MD, 1968 (Chapter 7).

[28] K. Kandori, N. Horigami, A. Yasukawa, T. Ishikawa, Texture and formation mechanism of fibrous calciumhydroxyapatite particles prepared by decomposition of calcium–EDTE Chelates,J. Am. Ceram. Soc. 80 (1997) 1157–2916.

[29] W. Harris, N. White, X-ray Diffraction Techniques for Soil Mineral Identification, Chapter 4, Methods of Soil Analysis, Part 5. Mineralogical Methods. SSSA Book Series, no. 5. Soil Science Society of America, 677 S. Segoe Road, Madison, WI 53711, USA, (2007) pp. 23.

[30] D. Tadic, M. Epple, A thorough physicochemical characterization of 14 calcium phosphate-based bone substitution materials in comparison to natural bone, Biomaterials 25 (2004) 987–994.

[31] G. Couarraze, J.L. Grossiord, Initiation à la rhéologie (Introduction to Rheology), Technique et Documentation, Lavoisier, Paris, 1983.

[32] J.J. Porter, S. Zhuang, Microfiltration of sodium nitrate and Direct Red 2 dye using asymmetric titanium dioxide membranes on porous ceramic tubes, J. Membr. Sci. 110 (1996) 119–132.

[33] M. Khemakhem, S. Khemakhem, S. Ayedi, M. Cretin, R. Ben Amar, Development of an asymmetric ultrafiltration membrane based on phosphates industry sub-products, Ceram. Int., 41 Part A (2015) 10343–10348.

[34] G. Masmoudi, E. Ellouze, R. Ben Amar, Hybrid coagulation/membrane process treatment applied to the treatment of industrial dyeing effluent, Desalin. Water Treat. 57 (2016) 6781–6791